

# Characterization and modelling of K<sub>2</sub>CO<sub>3</sub> cycles for thermochemical energy storage applications

**Citation for published version (APA):**

Beving, M., Frijns, A., Rindt, C., & Smeulders, D. (2019). *Characterization and modelling of K<sub>2</sub>CO<sub>3</sub> cycles for thermochemical energy storage applications*. Paper presented at Eurotherm Seminar 112- Advances in Thermal Energy Storage, Lleida, Spain.

**Document status and date:**

Published: 01/01/2019

**Document Version:**

Accepted manuscript including changes made at the peer-review stage

**Please check the document version of this publication:**

- A submitted manuscript is the version of the article upon submission and before peer-review. There can be important differences between the submitted version and the official published version of record. People interested in the research are advised to contact the author for the final version of the publication, or visit the DOI to the publisher's website.
- The final author version and the galley proof are versions of the publication after peer review.
- The final published version features the final layout of the paper including the volume, issue and page numbers.

[Link to publication](#)

**General rights**

Copyright and moral rights for the publications made accessible in the public portal are retained by the authors and/or other copyright owners and it is a condition of accessing publications that users recognise and abide by the legal requirements associated with these rights.

- Users may download and print one copy of any publication from the public portal for the purpose of private study or research.
- You may not further distribute the material or use it for any profit-making activity or commercial gain
- You may freely distribute the URL identifying the publication in the public portal.

If the publication is distributed under the terms of Article 25fa of the Dutch Copyright Act, indicated by the "Taverne" license above, please follow below link for the End User Agreement:

[www.tue.nl/taverne](http://www.tue.nl/taverne)

**Take down policy**

If you believe that this document breaches copyright please contact us at:

[openaccess@tue.nl](mailto:openaccess@tue.nl)

providing details and we will investigate your claim.



EUROTHERM112-S133

## Characterization and modelling of $K_2CO_3$ cycles for thermochemical energy storage applications

Max A.J.M. Beving<sup>1,\*</sup>, Arjan J.H. Frijns<sup>1</sup>, Camilo C.M. Rindt<sup>1</sup>, David M.J. Smeulders<sup>1</sup>

<sup>1</sup>Eindhoven University of Technology, Department of Mechanical Engineering, P.O. Box 513, 5600MB Eindhoven, The Netherlands

\*Corresponding author e-mail: [m.a.j.m.beving@tue.nl](mailto:m.a.j.m.beving@tue.nl)

### Abstract

Thermochemical heat storage in salt hydrates is a promising concept to bridge the gap between supply and demand of solar thermal energy in the built environment. Using a suitable thermochemical material (TCM), a heat battery can be created to supply low-temperature thermal energy during colder time periods. The principle is based on a reversible hydration-dehydration reaction with water vapour. The TCM can be charged (dehydrated) at a temperature of 120°C by using solar thermal collectors. Conversely, the discharge (hydration) occurs at room temperature using a constant water vapour pressure of 12 mbar. Previous studies have indicated that potassium carbonate ( $K_2CO_3$ ) is a good candidate to fulfil the role of TCM in built environment applications. To generate adequate power from a heat battery for hot tap water or space heating, the kinetics of the TCM need to be sufficiently fast. It is hypothesized that the kinetics of the material improve over multiple charge and discharge cycles due to crack formation and volume increase of the grains. The aim of this work is to evaluate the kinetics of 500-700  $\mu\text{m}$   $K_2CO_3$  grains using thermogravimetric analysis and differential scanning calorimetry (TGA/DSC), and to quantify the improvement in kinetics over multiple charge and discharge cycles. The kinetics serve as input for an existing nucleation and growth model, simulating the fractional conversion at grain level. In the TGA/DSC experiments, the material was charged and discharged numerous times under a constant water vapour pressure of 12 mbar. The cycling temperature varies from room temperature to a maximum temperature of 120°C. The conversion time of each cycle was monitored. Additionally, using an optical microscope, cycling experiments of  $K_2CO_3$  were performed in a micro climate chamber with the same conditions as in the TGA/DSC experiments. This allows tracking of the apparent surface area of the grains and the observation of crack formation for each cycle. The existing nucleation and growth model is enhanced by incorporating grain growth and crack formation observed from the optical experiments. Thermal characterization by means of TGA/DSC has indicated that indeed the kinetics of the material improve over multiple cycles. Typical conversion rates are increased by a factor 10 comparing the first and the 12<sup>th</sup> cycle. Preliminary optical microscope experiments show an increase of the apparent grain surface area of approximately 55%. Additionally, crack formation is observed over multiple hydration and dehydration cycles leading to increased inter-particle porosity, likely adding to the improved kinetics.

**Keywords:** Thermochemical heat storage, Nucleation and Growth model, TGA/DSC, Heat Battery, Salt Hydrate

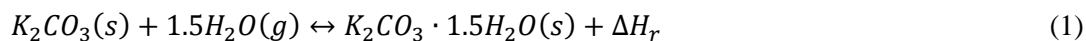


## 1. Introduction

Fossil fuel depletion and climate change are becoming increasingly hot topics in Europe. The European Commission roadmap has stated that it is necessary to reduce CO<sub>2</sub> emissions by 95% by 2050 compared to 1995. In the residential sector, 68% of the end-use energy is dedicated to space and water heating [1]. Solar energy is one of the most promising sustainable energy source to fulfil this heating demand. However, since solar energy is intermittent, long-term energy storage is required.

Thermal energy storage using thermochemical materials (TCMs) is a promising technique to store energy without significant losses, and over longer periods of time [2]. The principle of TCM storage involves a reversible chemical reaction between a solid and a gas. The reaction is described according to  $A(s) + B(g) \leftrightarrow AB(s) + \text{heat}$ . Charging the TCM requires adding heat to the system, expelling the gas and therefore storing the added heat. Recombining the gas and the TCM releases the heat. This work focuses on a water-salt-hydrate reaction pair, which is suitable for low-temperature heat storage [3]. Dwellings equipped with solar panels can apply the acquired heat during summer to dehydrate the TCM. In colder periods, inducing water vapour to the dehydrated material frees the stored heat. This principle allows the creation of a heat battery.

Donkers et al. published a review on 563 thermochemical materials and included criteria such as operating conditions, costs and environmental impact [4]. One of the most promising salt hydrates according to this study is K<sub>2</sub>CO<sub>3</sub>. This material has a theoretical volumetric energy density of 1.3GJ/m<sup>3</sup> and its thermochemical reaction is given by:



with  $\Delta H_r$  the reaction enthalpy of 65.8kJ/mol of water.

Care should be taken when a TCM is hydrated as salt hydrates are prone to over-hydration [5], [6]. This phenomenon causes the micro pores of the material to saturate with crystal water. Dehydrating the material afterwards causes a non-porous structure that dramatically reduces water transport and hence the performance of the TCM. A phase diagram is commonly used to evaluate the operating conditions of a salt hydrate [7].

The performance of a TCM is hypothesized to improve due to the opposite effect of over-hydration: crack formation and consequentially volume growth of the particles. Multiple charge and discharge cycles cause the grains to break open, leading to an increase in micro porosity that allows water to enter and exit the sample more easily. The formation of micro-channels is demonstrated in [8] for the dehydration of lithium sulphate.

In order to improve existing thermochemical heat storage systems, a comprehensive understanding of the reaction kinetics is required. Numerical models describing the hydration and dehydration phenomena can be particularly helpful in this regard. Typical solid-state reaction models are available in the literature [9,10]. However, these analytical models are often used to evaluate the overall process and in several occasions even led to erroneous results. This is elaborated extensively in the works of Pijolat et al. and Favergeon et al. [11,12] and an alternative approach was proposed to kinetic modelling based on nucleation and growth. The dehydration of lithium sulphate monohydrate was studied using a nucleation and growth modelling approach [13,14]. The model is based on Mampel's assumptions and uses a stochastic approach to account for non-isothermal and non-isobaric conditions [15]. Moreover, this model is applicable to any grain shape.

In present work, the nucleation and growth model created by Lan et al. [13] is extended to include grain growth and the formation of cracks in K<sub>2</sub>CO<sub>3</sub> grains. The effect is investigated of these morphological changes on the kinetics. Microscopy experiments on K<sub>2</sub>CO<sub>3</sub> particles are performed to evaluate the grain growth as function of the amount of charge and discharge cycles. TGA/DSC experiments are performed in parallel to evaluate the performance of the material under the same conditions as the microscopy experiments. This way the hypothesis is tested that

grain growth and consequentially crack formation go hand-to-hand with the improvement of TCM performance.

## 2. Materials and Methods

To provide input to the numerical model, two types of experiments are carried out. The microscopy experiments are used to evaluate the geometrical changes of the particles as function of the number of cycles. TGA/DSC experiments allow the determination of the fractional conversion, power output and energy content of the grains. In these experiments,  $K_2CO_3$  particles (Sigma-Aldrich, 700 – 1000  $\mu\text{m}$  in diameter) were used. The particles were stored in a small closed container to prevent over-hydration (possibly causing deliquescence) or dehydration.

### *Microscopy experiments*

$K_2CO_3$  particles are placed in a so-called ‘stage’, which is a miniature climate chamber (Linkam THMS600-H Stage) that is connected to a humidifier (Linkam RH95). The humidity and temperature are carefully controlled by the humidifier and the stage. The particle environment is alternated between hydration and dehydration conditions. The operating conditions are set according to the phase diagram, to ensure that the sample conditions are below deliquescent conditions at all times. More details on the pressure and temperature conditions for  $K_2CO_3$  can be found in [7]. A typical example of the grains evaluated from the micro climate chamber is shown in Figure 1.

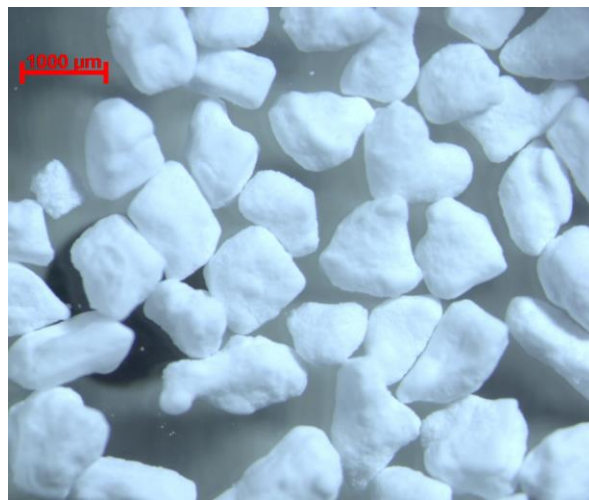


Figure 1: Typical example of  $K_2CO_3$  grains in the micro climate chamber.

One very important factor to consider is the sample mass. Based on previous work [6,16,17] it is concluded that the sample mass should be kept small. The ratio of diffusion over intrinsic reaction rate decreases as sample mass decreases (assuming the same particle size). A small sample mass ensures a good representation of the hydration reaction. The typical sample mass used is 10 mg. By sample mass is meant the number of particles times the averaged mass of an individual particle. The average mass of 1 grain is 0.285mg.

First, the sample is dehydrated by increasing the stage temperature from 25  $^{\circ}\text{C}$  to 120  $^{\circ}\text{C}$  using a heating rate of 1 K/min and setting the RH to 2% @ 25  $^{\circ}\text{C}$ . This translates to a water vapour pressure of approximately 32 Pa, or 0.32 mbar. During the first dehydration, these conditions are maintained for at least 10 hours to ensure that the sample is completely dehydrated.

After this initial dehydration, the sample is cooled to 25  $^{\circ}\text{C}$  with a cooling rate of 1 K/min, in dry conditions. Once this temperature is reached these conditions are kept constant for 40 minutes to allow a stable environment. Afterwards, the RH is set to 38 % at 25  $^{\circ}\text{C}$ , which is equivalent to a



water vapour pressure of 12 mbar. This initiates the hydration process and the sample is hydrated for 10 hours. Subsequent dehydrations are done for 3 hours. Dehydration and hydration cycles are alternated for at least 12 cycles. Every 10 minutes, a picture of the sample (Figure 1) was taken using the Zeiss microscope (SteREO Discovery V20). This allows the observation of morphological changes of the sample particles. The particle growth is measured and averaged over 10 particles, mapping the growth of the particles as function of the number of cycles.

### *TGA/DSC experiments*

Additional experiments using a thermogravimetric, differential scanning calorimetric analyser (TGA/DSC, Jupiter F3 STA 449) were performed. This allows careful monitoring of the sample weight (TGA) and the heat flux (DSC). Characterization of materials by means of TGA/DSC is up to the present a widely applied technique [6,7,18–21].

The TGA/DSC experiments are performed at the same conditions as the optical microscope experiments. A typical sample mass of approximately 10mg was loaded in aluminium pans of 40  $\mu$ L without a lid and placed in the furnace. The material was then cycled 12 times. A ProUmid MHG Modular Humidity Generator with a flow rate of 300 ml/min and 38 % RH at 25°C, or 12 mbar, is used to hydrate the sample. The measured sample masses are translated to the fractional conversion by:

$$\alpha(t) = \frac{m_0 - m(t)}{m_0 - m_\infty} \quad (2)$$

in which  $\alpha(t)$  is the fractional conversion as function of time,  $m_0$  is the initial mass of the sample,  $m(t)$  the mass at time  $t$  and  $m_\infty$  the final mass of the sample. The conversion ranges from 0, indicating that the reaction is yet to start, to 1 which indicates that the reaction is completed. The TGA/DSC apparatus was calibrated before the experiments were performed.

### *Nucleation and growth model*

The nucleation and growth model consists of a spherical geometry with initial radius  $R_0$ . The sphere is represented by  $N$  randomly generated discrete points. Initially, the geometry is in an untransformed state (blue). When the simulation starts, nucleation is initiated on the boundary of the sphere causing nuclei to appear on the surface. Nucleation is followed by deterministic, isotropic growth towards the centre of the sphere. The radii of the nuclei grow with a constant growth rate  $\varphi$  [mol/m<sup>2</sup>s] according to:

$$r_n(\tau, t) = V_m \varphi (t - \tau) \quad (3)$$

With  $r_n(\tau, t)$  the radius [m] of a nucleus formed at time  $\tau$  [s] and evaluated at time  $t$  [s] ( $t \geq \tau$ ) and  $V_m$  the molar volume of the grain [m<sup>3</sup>/mol]. If the distance between a nuclei  $\sigma(x, y, z)$  formed on the surface and an arbitrary point  $p(x, y, z)$  in the bulk is covered by the radius of a nucleus, that area is transformed. This holds when:

$$\frac{(p_x - \sigma_x)^2 + (p_y - \sigma_y)^2 + (p_z - \sigma_z)^2}{r_n(\tau, t)^2} \leq 1 \quad (4)$$

With  $p_x$  the x-coordinate of point  $x$ ,  $\sigma_x$  the x-coordinate of point  $\sigma$  etc. The rate limiting step is assumed to be at the interface between the initial phase and the new phase of the sphere. Simulation snapshots of the nucleation and growth process are displayed in Figure 2.



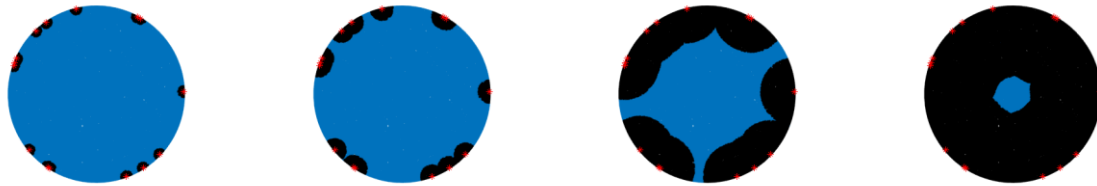


Figure 2: Simulation snapshots of the nucleation and growth model. Initially, the sphere is in an untransformed state (blue). After the simulation starts, nuclei (in red) are formed on the surface area of the grain. Following the nucleation process, each nucleus grows towards the centre of the sphere. This growth is deterministic. Transformed areas are shown in black.

The fractional conversion is determined by calculating the ratio of transformed to total points, neglecting coalescence and ingestion. The radius  $R_0$  of the sphere is set to  $6 \cdot 10^{-4}$  m. The molar volume  $V_m$  is set to  $2.4 \cdot 10^{-6}$  [m<sup>3</sup>/mol].

Modelling the fractional conversion using a nucleation and growth approach has several advantages. It is applicable to any geometry shape and is valid for non-isothermal and non-isobaric conditions. In this work the nucleation rate is assumed to be very high. This activates all surface points for nucleation instantaneously, covering the surface area of the sphere by a thin layer of product. This results in a model resembling a shrinking core characteristic. The fractional conversion is therefore only dependent on the growth rate and the surface area available for nucleation.

#### Crack formation

Due to repeated hydration and dehydration of the material, the TCM is expected to crack and expand in volume. The numerical model is adjusted accordingly by introducing cracks and allowing the grains to grow in size with each cycle. The cracks are assumed to be straight and split the sphere all the way to the core to avoid complexity. Simulation snapshots of the sphere with different amount of cracks are displayed in Figure 3. The radius of the particle increases with each crack such that the total solid volume,  $V_{solid} = V_{sphere} - V_{pores}$ , remains constant.

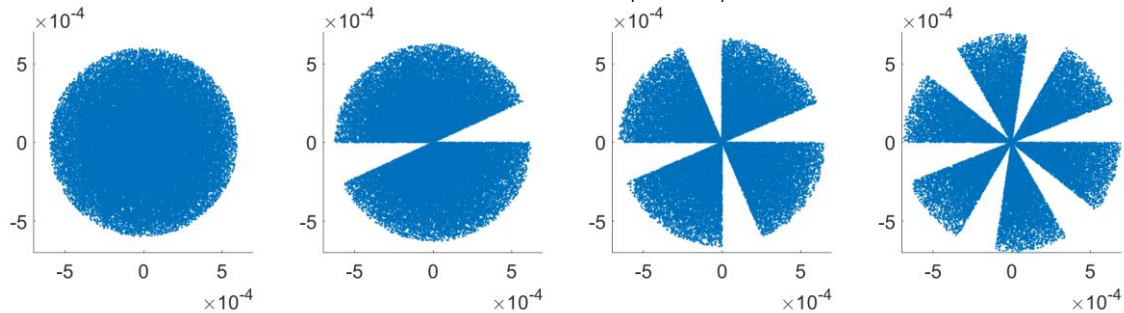


Figure 3: Simulation snapshots of the geometry adapted with cracks. The particle radius increases as the amount of cracks increases.

### 3. Results and discussion

In this section, the results of the microscopy experiments, the TGA/DSC experiments and the numerical simulations are shown and discussed.

#### Microscopy experiments

$K_2CO_3$  particles were cycled 12 times and pictures of the top view of the individual particles were taken after each hydration cycle. This ‘projected area’ was averaged over 10 particles after each hydration, and the results are displayed in Figure 4.

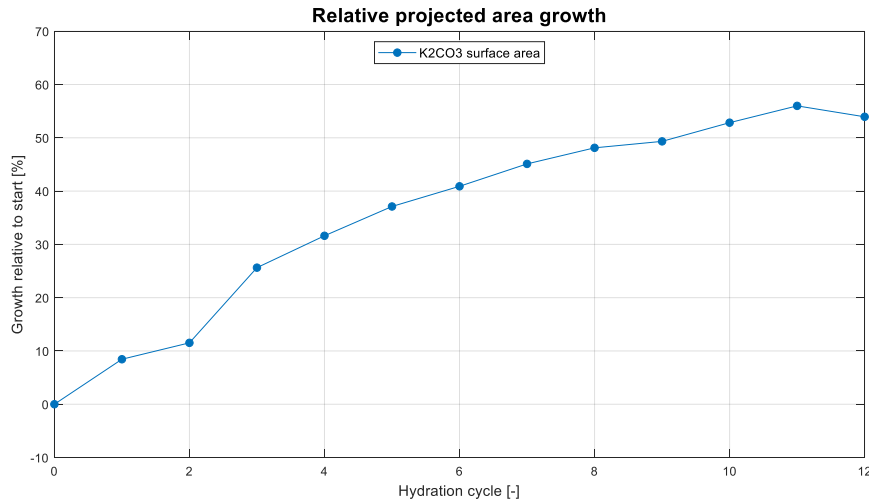


Figure 4: Relative growth of the projected area of the grains of a 10mg sample. The percentage area increase is relative to the initial area.

It is observed that the relative area increases after each hydration until a limit is reached. On average, the relative area is increased by 7% compared to the initial size. A maximum increase of about 55% is observed after hydration 12.

#### TGA/DSC experiments

A 10 mg sample of  $K_2CO_3$  was cycled 12 times in a TGA measuring device, and the conversion was monitored. The maximum hydration time is set to 10 hours (36000 seconds). The results are displayed in Figure 5. The TGA results show that cycle 1 does not reach full conversion in 10 hours. Although initially the conversion increases rapidly, it levels off as the experiment progresses. However after subsequent cycles, a significant increase in conversion speed is observed, likely due to grain growth and consequently crack formation. This improvement continues until the 12<sup>th</sup> cycle, which is completed after only 45 minutes. The improvement in conversion speed is diminished over time. This indicates that the effect of grain growth and crack formation on the reduction in hydration time becomes less significant with each cycle.

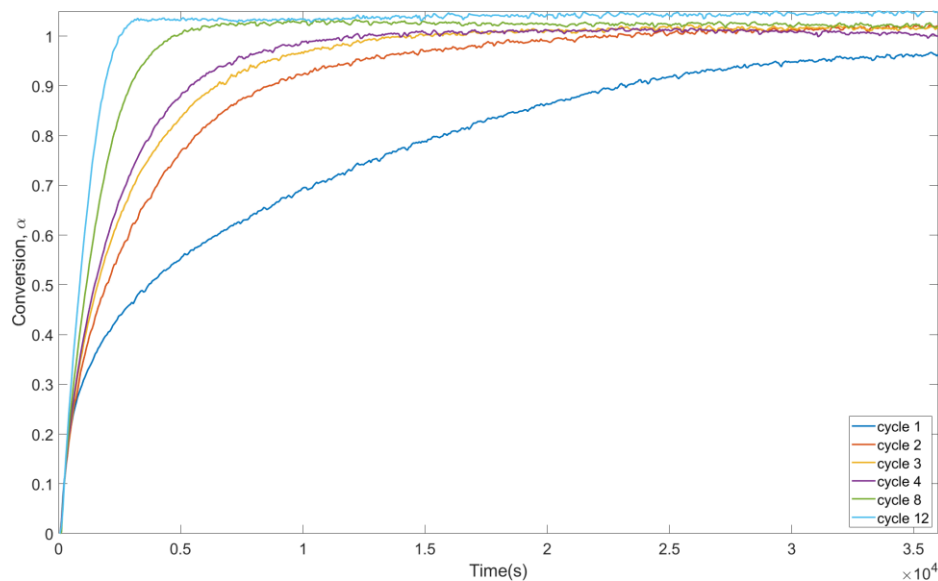


Figure 5: Conversion of the hydration of a 10mg  $K_2CO_3$  sample. It is observed that the first hydration cycle (dark blue) does not reach full conversion in 10 hours. After subsequent hydration cycles, however, the reaction speed is increased.

### *Nucleation and Growth model*

The numerical results of the nucleation and growth model are displayed and discussed in this section. It is assumed that the particles have not yet developed any cracks during the first cycle. First, a sphere without any cracks is simulated and the conversion is compared to the TGA result of the first cycle. It is assumed that all surface points are activated and start to grow immediately after the simulation starts. Observing the fast increase in conversion for lower time steps (Figure 5) this assumption seems valid. The growth rate  $\varphi$  is fitted to cycle 1 of the TGA result. This results in a growth rate of  $\varphi = 3.1 \cdot 10^{-4} \text{ mol/m}^2\text{s}$ . The result is displayed in Figure 6.

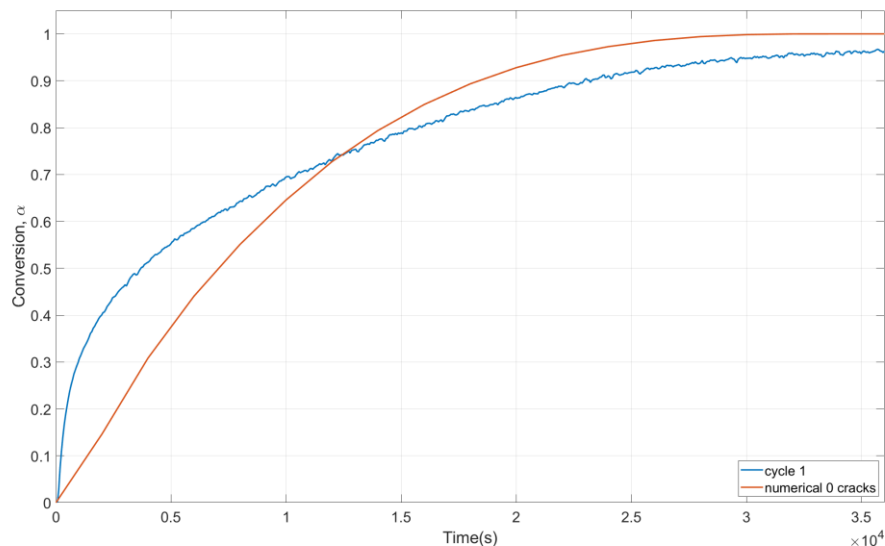


Figure 6: Numerical simulation of a spherical geometry without cracks in orange. TGA result of a 10mg sample in blue. The growth rate used in this simulation is  $\varphi = 3.1 \cdot 10^{-4} \text{ mol/m}^2\text{s}$ .

It is observed that the numerical model predicts a lower wetting rate than observed in the experiments. The mismatch between numerical simulations and experiments may be explained by the hypothesis that the rate limiting step is at the interface. In the experiment the material is hydrated quickly up to a conversion of 0.3. As the reaction proceeds, the fractional conversion increases more slowly as water needs to diffuse into the bulk material. This may indicate that a later stages of the conversion the limiting step becomes the diffusion of water into the bulk.

Next, the effect of the cracks on the fractional conversion was simulated. The growth rate is kept constant at  $\varphi = 3.1 \cdot 10^{-4} \text{ mol/m}^2\text{s}$  and for every cycle 2 extra cracks (Figure 3) are introduced. This is done to avoid asymmetry affecting the fractional conversion. The result is displayed in Figure 7.



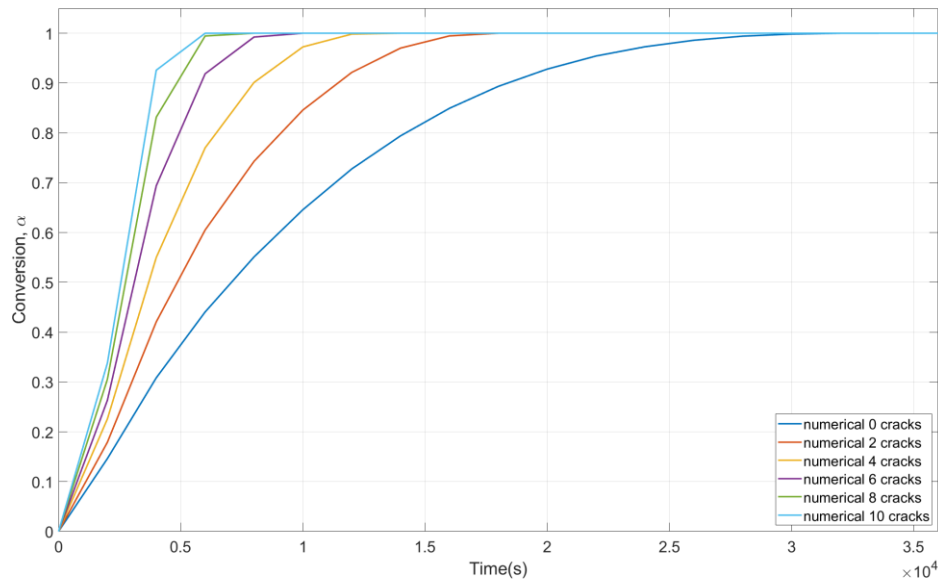


Figure 7: Modelled fractional conversion with a constant growth rate of  $3.1 \cdot 10^{-4} \text{ mol/m}^2\text{s}$  and an increasing amount of cracks. The time step of the simulation was 2000s.

The same trend is observed as in the TGA experiments: the more cracks are introduced, the faster full conversion goes. Water can access untransformed material easier because it can diffuse through the air in between the cracks as opposed to diffusion through the bulk material. Indeed the model shows that an increase in number cracks improves the hydration time.

## Conclusion

In this work a hypothesis is posited that grain growth and consequentially crack formation go hand-to-hand with the improvement of a TCM. To this end, a  $K_2CO_3$  sample was cycled in a micro climate chamber while carefully monitoring the temperature and humidity. Using an optical microscope, pictures of the particles were taken at regular intervals. This allows tracking of the projected surface area and hence, the increase of the particle radius. After 12 cycles, the apparent surface area is increased by approximately 55%. This confirms the hypothesis that the particles grow in size and cracks are formed in the grain structure.

$K_2CO_3$  particles were cycled 12 times in a TGA measurement device and the fractional conversion was monitored over time. The first cycle reached only 95% of the full conversion after 10 hours. Subsequent cycling dramatically reduced the conversion time from 10+ hours of the first cycle, down to 45 minutes for the 12<sup>th</sup> cycle. It is concluded that repeated thermal cycling of  $K_2CO_3$  particles can potentially reduce the hydration time by a factor 10-12. Combined with the microscopy results, it is concluded that the increase in particle volume and formation of cracks in the particles the main reason of the reduced hydration time.

A numerical model based on nucleation and growth phenomena was modified to include crack formation and grain growth. The nucleation rate is assumed to be very high: instant activation of all surface points of the grains with an isotropical growth towards the centre. The growth rate  $\varphi$  is fitted with TGA data of the first  $K_2CO_3$  cycle. In every next cycle, the number of cracks is increased by 2. The same growth rate as in cycle 1 is assumed. The numerical results underestimate the initial fractional conversion, but overall the trend of improvement in kinetics caused by the increased surface area is present in both numerical and experimental results.

Improvements to the hydration time of a TCM can be made by introducing micro cracks to the TCM grains. This allows the water to diffuse into the material easier at the start of the experiment.



## Acknowledgements

This project is sponsored by the Advanced Dutch Energy Material (ADEM) program. The authors would like to thank Casper Jansen and Daniël Lelivelt for their contribution to the experimental and numerical results respectively.

## References

- [1] Quadrelli R. Energy efficiency indicators - highlights. 2017.
- [2] N'Tsoukpoe KE, Liu H, Le Pierrès N, Luo L. A review on long-term sorption solar energy storage. *Renew Sustain Energy Rev* 2009;13:2385–96. doi:10.1016/j.rser.2009.05.008.
- [3] N'Tsoukpoe KE, Schmidt T, Rammelberg HU, Watts BA, Ruck WKL. A systematic multi-step screening of numerous salt hydrates for low temperature thermochemical energy storage. *Appl Energy* 2014;124:1–16. doi:10.1016/j.apenergy.2014.02.053.
- [4] Donkers, P.A.J. Sögütoglu LC. A review of salt hydrates for seasonal heat storage in domestic applications. *Appl Energy* 2017;199:45–68. doi:https://doi.org/10.1016/j.apenergy.2017.04.080.
- [5] Ferchaud CJ. Experimental study of salt hydrates for thermochemical seasonal heat storage. vol. 5. 2016.
- [6] Gaeini M, Rouws AL, Salari JWO, Zondag HA, Rindt CCM. Characterization of microencapsulated and impregnated porous host materials based on calcium chloride for thermochemical energy storage. *Appl Energy* 2018;212:1165–77. doi:10.1016/j.apenergy.2017.12.131.
- [7] Sögütoglu LC, Donkers PAJ, Fischer HR, Huinink HP, Adan OCG. In-depth investigation of thermochemical performance in a heat battery: Cyclic analysis of K<sub>2</sub>CO<sub>3</sub>, MgCl<sub>2</sub> and Na<sub>2</sub>S. *Appl Energy* 2018;215:159–73. doi:10.1016/j.apenergy.2018.01.083.
- [8] Galwey AK, Koga N, Tanaka H. A kinetic and microscopic investigation of the thermal dehydration of lithium sulphate monohydrate. *J Chem Soc Faraday Trans* 1990;86:531–7. doi:10.1039/FT9908600531.
- [9] Khawan A, Flanagan RD. Solid-State kinetic Models: Basic and Mathematical Fundamentals. *JPhysChemB* 2006;110:17315–28. doi:10.1021/jp062746a.
- [10] Galwey AK, Brown ME. Thermal Decomposition of Ionic Solids. 1999.
- [11] Michèle P, Loïc F, Michel S. From the drawbacks of the Arrhenius-f( $\alpha$ ) rate equation towards a more general formalism and new models for the kinetic analysis of solid-gas reactions. *Thermochim Acta* 2011;525:93–102. doi:10.1016/j.tca.2011.07.026.
- [12] Favergeon L, Morandini J, Pijolat M, Soustelle M. A General Approach for Kinetic Modeling of Solid-Gas Reactions at Reactor Scale: Application to Kaolinite Dehydroxylation. *Oil Gas Sci Technol – Rev d'IFP Energies Nouv* 2013;68:1039–48. doi:10.2516/ogst/2012018.
- [13] Lan S, Zondag H, Van Steenhoven A, Rindt C. Kinetic study of the dehydration reaction of lithium sulfate monohydrate crystals using microscopy and modeling. *Thermochim Acta* 2015;621:44–55. doi:10.1016/j.tca.2015.10.005.
- [14] Favergeon L, Pijolat M, Valdivieso F, Helbert C. Experimental study and Monte-Carlo simulation of the nucleation and growth processes during the dehydration of Li<sub>2</sub>SO<sub>4</sub>·H<sub>2</sub>O single crystals. *Phys Chem Chem Phys* 2005;7:3723–7. doi:10.1039/b507644g.
- [15] Helbert C, Touboul E, Perrin S, Carraro L, Pijolat M. Stochastic and deterministic models for nucleation and growth in non-isothermal and/or non-isobaric powder transformations. *Chem Eng Sci* 2004;59:1393–401. doi:10.1016/j.ces.2003.12.004.
- [16] Lan S, Zondag H, van Steenhoven A, Rindt C. An experimentally validated numerical model of interface advance of the lithium sulfate monohydrate dehydration reaction. *J Therm Anal Calorim* 2016;124:1109–18. doi:10.1007/s10973-015-5210-z.
- [17] Lan S, Gaeini M, Zondag H, Steenhoven A Van, Rindt C. Direct numerical simulation of



- the thermal dehydration reaction in a TGA experiment. *Appl Therm Eng* 2018;128:1175–85. doi:10.1016/j.applthermaleng.2017.08.073.
- [18] Vyazovkin S, Chrissafis K, Di Lorenzo ML, Koga N, Pijolat M, Roduit B, et al. ICTAC Kinetics Committee recommendations for collecting experimental thermal analysis data for kinetic computations. *Thermochim Acta* 2014;590:1–23. doi:10.1016/j.tca.2014.05.036.
- [19] Vyazovkin S, Burnham AK, Criado JM, Pérez-Maqueda LA, Popescu C, Sbirrazzuoli N. ICTAC Kinetics Committee recommendations for performing kinetic computations on thermal analysis data. *Thermochim Acta* 2011;520:1–19. doi:10.1016/j.tca.2011.03.034.
- [20] Brancato V, Calabrese L, Palomba V, Frazzica A, Fullana-Puig M, Solé A, et al. MgSO<sub>4</sub>·7H<sub>2</sub>O filled macro cellular foams: An innovative composite sorbent for thermochemical energy storage applications for solar buildings. *Sol Energy* 2018;173:1278–86. doi:10.1016/j.solener.2018.08.075.
- [21] Solé A, Martorell I, Cabeza LF. State of the art on gas-solid thermochemical energy storage systems and reactors for building applications. *Renew Sustain Energy Rev* 2015;47:386–98. doi:10.1016/j.rser.2015.03.077.